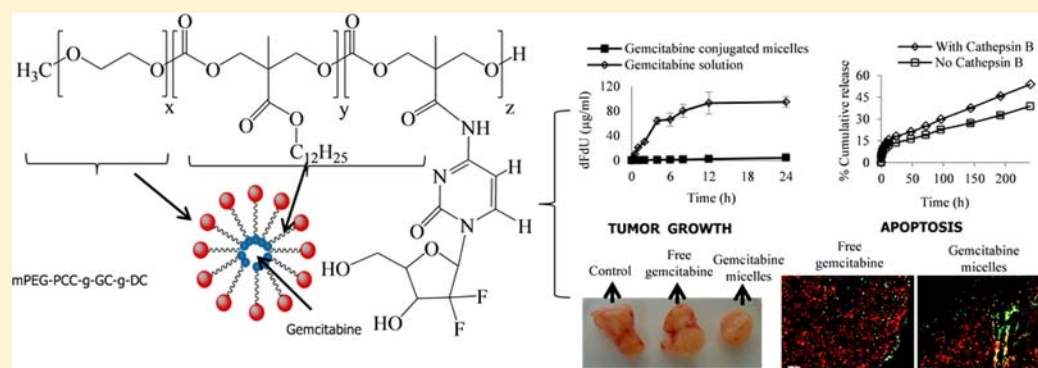


## Self-Assembling, Amphiphilic Polymer–Gemcitabine Conjugate Shows Enhanced Antitumor Efficacy Against Human Pancreatic Adenocarcinoma

Deepak Chitkara,<sup>§,†</sup> Anupama Mittal,<sup>§</sup> Stephan W. Behrman,<sup>‡</sup> Neeraj Kumar,<sup>†</sup> and Ram I. Mahato<sup>\*,§</sup>

<sup>§</sup>Department of Pharmaceutical Sciences and <sup>‡</sup>Department of Surgery, University of Tennessee Health Science Center, Memphis, Tennessee 38163, United States

<sup>†</sup>Department of Pharmaceutics, National Institute of Pharmaceutical Education and Research, S.A.S. Nagar, India 160062



**ABSTRACT:** The therapeutic efficacy of gemcitabine is severely compromised due to its rapid plasma metabolism. Moreover, its hydrophilicity poses a challenge for its efficient entrapment in nanosized delivery systems and to provide a sustained release profile. In this study, gemcitabine was covalently conjugated to poly(ethylene glycol)-*block*-poly(2-methyl-2-carboxyl-propylene carbonate) (PEG-PCC) which could self-assemble into micelles of 23.6 nm. These micelles afforded protection to gemcitabine from plasma metabolism as evident by negligible amount of gemcitabine and its metabolite dFdU detected in the plasma after 24 h. A controlled release of gemcitabine from the micelles was observed with 53.89% drug release in 10 days in the presence of protease enzyme Cathepsin B. Gemcitabine conjugated micelles were cytotoxic, showed internalization, and induced cell apoptosis in MIA PaCa-2 and L3.6pl pancreatic cancer cell lines. These micelles efficiently inhibited tumor growth when injected intravenously into MIA PaCa-2 cell derived xenograft tumor bearing NSG mice at a dose of 40 mg/kg in terms of reduced tumor volume and tumor weight (0.38 g vs 0.58 g). TUNEL assay revealed that gemcitabine conjugated micelles induced a much higher extent of apoptosis in the tumor tissues compared to free gemcitabine. In conclusion, gemcitabine conjugated micelles were able to enhance the drug payload, protect it from rapid plasma metabolism, and provide a sustained release and showed enhanced antitumor activity, and thus have the potential to provide a better therapeutic alternative for treating pancreatic cancer.

### INTRODUCTION

Pancreatic ductal adenocarcinoma is the fourth leading cause of cancer-related deaths, with only 3% of patients surviving for 5 years.<sup>1</sup> Surgical resection of the tumor is the only reliable treatment modality; however, prognosis still remains poor due to its potential for metastatic spread, high local recurrence, and chemoresistance, largely due to the presence of cancer stem cells.<sup>2–4</sup> Consequently, the need for chemotherapeutic strategies is of paramount importance.

Gemcitabine (2'-deoxy-2',2'-difluorocytidine) is a pyrimidine antimetabolite that displays anticancer activity by inducing S-phase arrest and inhibiting DNA synthesis.<sup>5,6</sup> Gemcitabine (Gemzar) is used as the first-line therapy for treating pancreatic ductal carcinoma; however, its clinical benefit is limited due to its short plasma half-life resulting from rapid metabolism by cytidine deaminase, into its inactive metabolite 2',2'-difluorodeoxyuridine (dFdU).<sup>7</sup> Its therapeutic efficacy is further diminished by its

hydrophilic nature which inhibits a high payload and prolonged drug release. Moreover, due to its hydrophilicity, its extravasation into the pancreatic cancer tissues which have a very dense fibrotic stroma is restricted. This compels a high dosing frequency at high drug doses which in turn precipitates significant adverse effects. To overcome these limitations, several derivatives/conjugates of gemcitabine and new delivery systems have been designed for its effective delivery into the tumor compartment.

Liposomes,<sup>8–11</sup> nanoparticles,<sup>12–15</sup> lipidic and nonlipidic derivatives, and polymeric drug conjugates<sup>5,16,17</sup> have been investigated to prevent rapid plasma degradation of gemcitabine and enhance delivery to the tumor tissue. Its liposomal formulation showed an appreciable improvement in its cytotoxic

Received: January 16, 2013

Revised: June 7, 2013

Published: June 13, 2013

activity against multiple myeloma<sup>11</sup> and human pancreatic cancer cell lines<sup>8</sup> along with an increase in half-life and area under the curve (AUC) in animal studies.<sup>18</sup> However, gemcitabine being a low molecular weight, uncharged molecule at physiological pH readily diffused out from the liposomal bilayers resulting in low entrapment efficiencies and rapid release rate.<sup>8</sup> Biodegradable poly( $\epsilon$ -caprolactone) nanoparticles containing magnetite and gemcitabine also showed promising results in xenograft models.<sup>12,15</sup> Nevertheless, these reported systems either have low drug encapsulation efficiencies due to high water solubility of gemcitabine or posed a problem of rapid drug release owing to faster drug diffusion from the system into the external aqueous environment.

Conjugating gemcitabine directly onto the lipidic or polymeric carrier has provided greater therapeutic advantage. Prodrugs of gemcitabine were synthesized by conjugating the lipidic chains at 3' and/or 5' hydroxyl and/or 4-amino group of gemcitabine.<sup>19–25</sup> These lipophilic prodrugs were shown to prevent degradation of gemcitabine by water as well as by metabolic enzymes. However, their low aqueous solubility necessitated their formulation into nanoparticles or lipid based carriers.<sup>26–28</sup> To meet this end, squalenoyl derivatives of gemcitabine were explored that self-assembled to form nanoparticles in aqueous media and showed superior anticancer activity as compared with free gemcitabine in 60 human tumor cell panel and subcutaneously grafted L1210 tumor models.<sup>23</sup> Although these nano-assemblies exhibited better pharmacokinetic profiles, their efficacy was limited by the rapid reticulo-endothelial system (RES) uptake because of hydrophobic surface and colloidal nature.<sup>22</sup> To reduce opsonization and blood clearance of these nano-assemblies, the PEGylation approach was used wherein poly(ethylene glycol)-cholesterol (PEG-chol) or squalene-PEG was added to form composite nano-assemblies and this was accompanied by a significant decrease in gemcitabine loading; however, addition of PEG showed enhanced efficacy on gemcitabine-resistant leukemia L1210K cells than either of the non-PEGylated counterparts or free gemcitabine.<sup>29</sup> In the present study, the presence of PEG corona ensures stealth properties of gemcitabine conjugated polymeric micelles while the presence of carboxyl groups enable the conjugation of higher content of gemcitabine to the polymer resulting in higher payload of gemcitabine. The current approach is so designed that it could be further exploited for co-delivery of multiple chemotherapeutic drugs,<sup>30</sup> since the polymer bears multiple carboxylic groups. This will help us achieve higher efficacy or overcome chemoresistance which might not be feasible in the previous system.

Polymeric conjugates of gemcitabine have been prepared using PEG,<sup>5,6</sup> poly(*N*-hydroxyethyl acrylamide) (PHEA),<sup>17</sup> polyglutamic acid,<sup>16,31</sup> and poly(*N*-(2-hydroxypropyl)methacrylamide) (HPMA).<sup>32</sup> PEG conjugates of gemcitabine have shown to improve the stability and its pharmacokinetic profile and enhance cytotoxicity.<sup>5,6</sup> However, PEG provides only one reactive functional group for conjugation with gemcitabine thus resulting in a reduced payload. To increase the payload, a bicarboxylic amino acid, aminoadipic acid, was used as a linker wherein a drug loading of 6.39% w/w was obtained.<sup>5</sup> Polyglutamic acid when conjugated to gemcitabine showed improved stability<sup>16</sup> and *in vivo* antitumor efficacy in breast tumor bearing mice.<sup>31</sup> Similar advantages of conjugation were also demonstrated by Yang et al.<sup>32</sup> and Cavallaro et al.<sup>17</sup> for HPMA and PHEA conjugates, respectively. In another study, hydrazone bonds were incorporated in the hydrophilic PEG and hydrophobic stearic acid to

form stimulus-sensitive micelles for lysosomal delivery. These micelles have been used for loading 4-(*N*)-stearoyl gemcitabine, a lipophilic prodrug.<sup>33</sup> Thus, this system is suitable only for hydrophobic drugs.

In our previous publications,<sup>34–36</sup> we used a copolymer of mPEG and MBC/PCC for delivery of hydrophobic drugs which get solubilized in the core of the micelles. However, the current work focuses on delivery of hydrophilic drug, gemcitabine, which itself is a challenging molecule for encapsulation in a nanocarrier system since it shows low payloads in nanocarriers and is prone to plasma metabolism. In this study, we have conjugated gemcitabine to the carboxyl pendant groups of poly(ethylene glycol)-*block*-poly(2-methyl-2-carboxyl-propylene carbonate) (PEG-PCC) thus enabling its efficient loading and improving the plasma stability. This polymer consists of two components, a biocompatible PEG block and a biodegradable polycarbonate PCC block. For the carbonate block, the starting monomer used is 5-methyl-5-benzoyloxycarbonyl-1,3-dioxane-2-one carbonate which is a modification of an intermediate used in the synthesis of numerous antiviral compounds. This polymer was chosen since polycarbonates possess biodegradability, low toxicity, and tunable mechanical properties. Furthermore, they degrade into carbon dioxide and alcohol, which unlike the degradation products of more frequently used polymers like poly(L-lactide) are less acidic, have less effect on microenvironment pH, and as such will not result in local inflammation.<sup>36–38</sup> Further, this amphiphilic copolymer self-assembles into micelles which were characterized for plasma stability, drug release, *in vitro* cytotoxicity, intracellular fate, and ability to induce apoptosis in MIA PaCa-2 pancreatic cancer cells and subsequently tested *in vivo* in MIA PaCa-2 cell derived xenograft tumor model after intravenous administration.

## ■ EXPERIMENTAL PROCEDURES

**Materials.** Gemcitabine hydrochloride was purchased from LC Laboratories (Woburn, MA) and tetrahydropyridine was purchased from Biovision. 2'-Deoxycytidine, Cathepsin B (5 U/mL), 2,2-bis(hydroxymethyl) propionic acid, methoxy polyethylene glycol (mPEG; Mn = 5000, polydispersity index (PDI) = 1.03), stannous 2-ethylhexanoate (Sn(Oct)<sub>2</sub>), 1-(3-dimethylaminopropyl)-3-ethylcarbodiimide HCl (EDC), 1-hydroxybenzotriazole (HOBT), and benzyl bromide were purchased from Sigma-Aldrich (St. Louis, MO) and used as received. LysoTracker Red DND-99 was procured from Molecular Probes, Invitrogen. DeadEnd Fluorimetric TUNEL (Terminal deoxynucleotidyl Transferase Biotin-dUTP Nick End Labeling) system was purchased from Promega (Madison, WI). All other chemicals were of analytical grade.

**Methods. Synthesis and Characterization of Polymer Drug Conjugate. Synthesis of 2-Methyl-2-Benzoyloxycarbonyl-Propylene Carbonate (MBC).** To improve the delivery and stability of gemcitabine, amphiphilic polymer with carboxylic pendant groups was synthesized as reported earlier by our group.<sup>34,39</sup> Briefly, monomer, MBC, was synthesized in a two-step reaction, wherein a mixture of 2,2-bis(hydroxymethyl)propionic acid (0.168 mol) and potassium hydroxide (0.169 mol) was reacted with benzyl bromide (0.202 mol) in dimethylformamide (DMF; 125 mL) at 100 °C for 16 h. The solvent was removed from the reaction mixture under reduced pressure and the residue obtained was dissolved in ethyl acetate, washed with water, and dried over MgSO<sub>4</sub>. Ethyl acetate was then evaporated to yield a crude product, which was recrystallized from toluene to give pure benzyl-2,2-bis(methylol)propionate. In the second step, benzyl

2,2-bis(methylol)-propionate (0.05 mol) was dissolved in dichloromethane-pyridine mixture (6:1 v/v; 175 mL) and chilled to  $-78^{\circ}\text{C}$ . Triphosgene (25 mmol in dichloromethane) was then added dropwise to it over 1 h and the reaction was allowed to continue for additional 2 h at the room temperature, followed by quenching with saturated aqueous  $\text{NH}_4\text{Cl}$  solution (75 mL). The organic layer was subsequently washed thrice with hydrochloric acid (1 M, 100 mL) followed by saturated aqueous  $\text{NaHCO}_3$  (300 mL) and dried with  $\text{Na}_2\text{SO}_4$ . The organic layer was then evaporated under reduced pressure to give MBC as a crude product, which was further recrystallized from ethyl acetate.

**Synthesis of PEG-MBC.** Polymer, PEG-MBC, was synthesized by ring-opening polymerization of MBC and mPEG in the presence of stannous-2-ethyl hexanoate as a catalyst at  $130^{\circ}\text{C}$  for 16 h under reduced pressure. The crude polymer so obtained was dissolved in chloroform and purified by precipitation in hexane-diethyl ether mixture followed by drying under vacuum for 48 h.

**Hydrogenation of PEG-MBC.** Protective benzyl group of PEG-MBC was removed by hydrogenation to obtain free carboxyl group for subsequent conjugation. For this, PEG-MBC (1 g) was dissolved in a mixture of tetrahydrofuran and methanol (1:1; 12 mL) containing palladium on carbon (Pd/C) (200 mg) and charged with hydrogen at a pressure of 55 psi. Reaction was allowed to continue for 18 h following which Pd/C was removed by filtration and solvent was evaporated under reduced pressure to get PEG-PCC.

**Conjugation of Gemcitabine and Dodecanol onto PEG-PCC.** Gemcitabine and dodecanol were conjugated to the carbonyl groups of PEG-PCC polymer using carbodiimide coupling. For this, PEG-PCC (300 mg) was dissolved in 5 mL of DMF followed by addition of 223 mg of 1-hydroxybenzotriazole (HOBT in 1 mL DMF), 317 mg of 1-(3-dimethylaminopropyl)-3-ethylcarbodiimide HCl (EDC in 5 mL DMF) and 340  $\mu\text{L}$  of diisopropylethylamine (DIPEA). Gemcitabine hydrochloride and dodecanol were dissolved in DMF containing 20  $\mu\text{L}$  of DIPEA and added to the reaction mixture. The reaction was allowed to proceed for 48 h under nitrogen atmosphere at room temperature. After completion of the reaction, crude product was purified by precipitation in large excess of cold diethyl ether. The precipitate was then dissolved in chloroform and precipitated twice in cold isopropyl alcohol. The precipitate obtained was then dissolved in acetone and dialyzed against water and lyophilized to obtain mPEG-b-PCC-g-gemcitabine-g-dodecanol (mPEG-PCC-g-GC-g-DC).

**Characterization of Polymer and Polymer Drug Conjugate.**  $^1\text{H}$  NMR spectra were recorded on a Bruker (400 MHz,  $T = 25^{\circ}\text{C}$ ) using  $\text{DMSO}-d_6$  as a solvent in a chemical shift range of 0–12. FTIR of gemcitabine, PEG-PCC, and polymer drug conjugate was recorded on a Perkin-Elmer spectrometer in a frequency range of 650–4000  $\text{cm}^{-1}$ .

**Formulation Development.** Gemcitabine conjugated polymeric micelles were prepared by nanoprecipitation as described previously with slight modification.<sup>34</sup> Briefly, 20 mg of mPEG-b-PCC-g-GC-g-DC copolymer was dissolved in acetone (0.5 mL) and added to 2 mL of phosphate buffered saline (PBS; pH 7.4). Acetone was then evaporated under reduced pressure followed by centrifugation at 5000 g for 5 min and filtration through 0.22  $\mu\text{m}$  filter to obtain the micelles. To assess the physical entrapment of gemcitabine in micelles, mPEG-b-PCC-g-DC was prepared and gemcitabine was loaded into it using nanoprecipitation method at a theoretical loading of 12.8% w/w.

**Characterization of Gemcitabine–Polymer Conjugate Micelles. Particle Size and Zeta Potential.** Particle size and zeta potential were measured by using Malvern Zetasizer (Nano ZS series). Micelles (10 mg/mL) were taken in purified water and analyzed at a scattering angle of  $173^{\circ}$ . A total of 12 measurements were taken per sample with a time span of 10 s. Zeta potential of micelles was determined in terms of electrophoretic mobility by taking an average of 5 measurements per sample. Data of particle size and zeta potential are reported as the mean  $\pm$  SD of three independent samples.

**Particle Morphology (Transmission Electron Microscopy, TEM).** Polymer drug conjugate micelles were visualized using a JEM-100S (Japan) TEM. Micellar suspension was loaded onto copper grid and air-dried. It was stained with uranyl acetate (1% w/v) and visualized under TEM at magnifications ranging from 50K to 100K with an accelerating voltage set at 60 kV.

**Critical Micelle Concentration (CMC).** CMC of gemcitabine conjugated polymer was determined using pyrene as a hydrophobic fluorescent probe as described earlier.<sup>33</sup> The fluorescent intensity was recorded at an excitation wavelength of 338 and 333 nm and emission wavelength of 390 nm using SpectraMax M2/M2e spectrofluorimeter (Molecular Devices, Sunnyvale, CA). The CMC value was obtained from the plots of intensity ratio ( $I_{338}/I_{333}$ ) versus logarithm of polymer concentration as intersection point of two tangents drawn to the curve at high and low concentrations.

**Quantification of Gemcitabine Payload in Polymer Drug Conjugate.** To extract out the conjugated drug, formulation (10 mg) was prepared and subjected to alkaline hydrolysis in NaOH (1 N) at  $40^{\circ}\text{C}$  for 1 h as reported earlier<sup>6</sup> for PEG–gemcitabine conjugate formulation. Samples were then appropriately diluted and the content of gemcitabine was determined by HPLC-UV analytical method. Chromatography was performed on Inertsil ODS 3 column (4.5  $\times$  250 mm) using methanol and sodium acetate buffer (20 mM, pH-5.5) as a mobile phase at the ratio of 07:93. Injection volume was kept at 20  $\mu\text{L}$  and analysis was performed at 268 nm. Payload was calculated using eq 1. The stability of free gemcitabine was also tested at the alkaline hydrolysis conditions, i.e., 1 N NaOH at  $40^{\circ}\text{C}$  for 1 h to determine any degradation of drug.

$$\text{Payload} \left( \frac{\% \text{w}}{\text{w}} \right) = \frac{\text{Amount of drug loaded}}{\text{Total weight of formulation}} \times 100 \quad (1)$$

**In Vitro Release of Gemcitabine.** *In vitro* release of gemcitabine from polymer drug conjugate micelles was studied in the presence and absence of protease Cathepsin B (5 U/mL). Micelles formulated in PBS (1 mL; equivalent to 0.5 mg of gemcitabine) containing 20  $\mu\text{L}$  of enzyme were taken in a dialysis bag (molecular weight cutoff 2000 Da), clamped at both ends, and placed in aqueous buffer, PBS (pH 5.5 and 7.4; 5 mL). Samples (1 mL) were withdrawn at regular time intervals and replaced with an equivalent amount of the fresh media. The content of gemcitabine present in the samples was analyzed using HPLC-UV method as described in the previous section. Samples containing physically entrapped gemcitabine in mPEG-b-PCC-g-DC micelles and free gemcitabine were also kept as controls.

**Stability Study in Human Plasma.** Human plasma (0.5 mL) was taken in microcentrifuge tubes and polymer drug conjugate micelles (in PBS; equivalent to 0.2 mg of gemcitabine) or gemcitabine were added to each tube followed by incubation at  $37 \pm 0.1^{\circ}\text{C}$ . At regular time intervals, plasma samples were taken to which 10  $\mu\text{L}$  of tetrahydrouridine (10  $\mu\text{g}/\text{mL}$ ) was added to

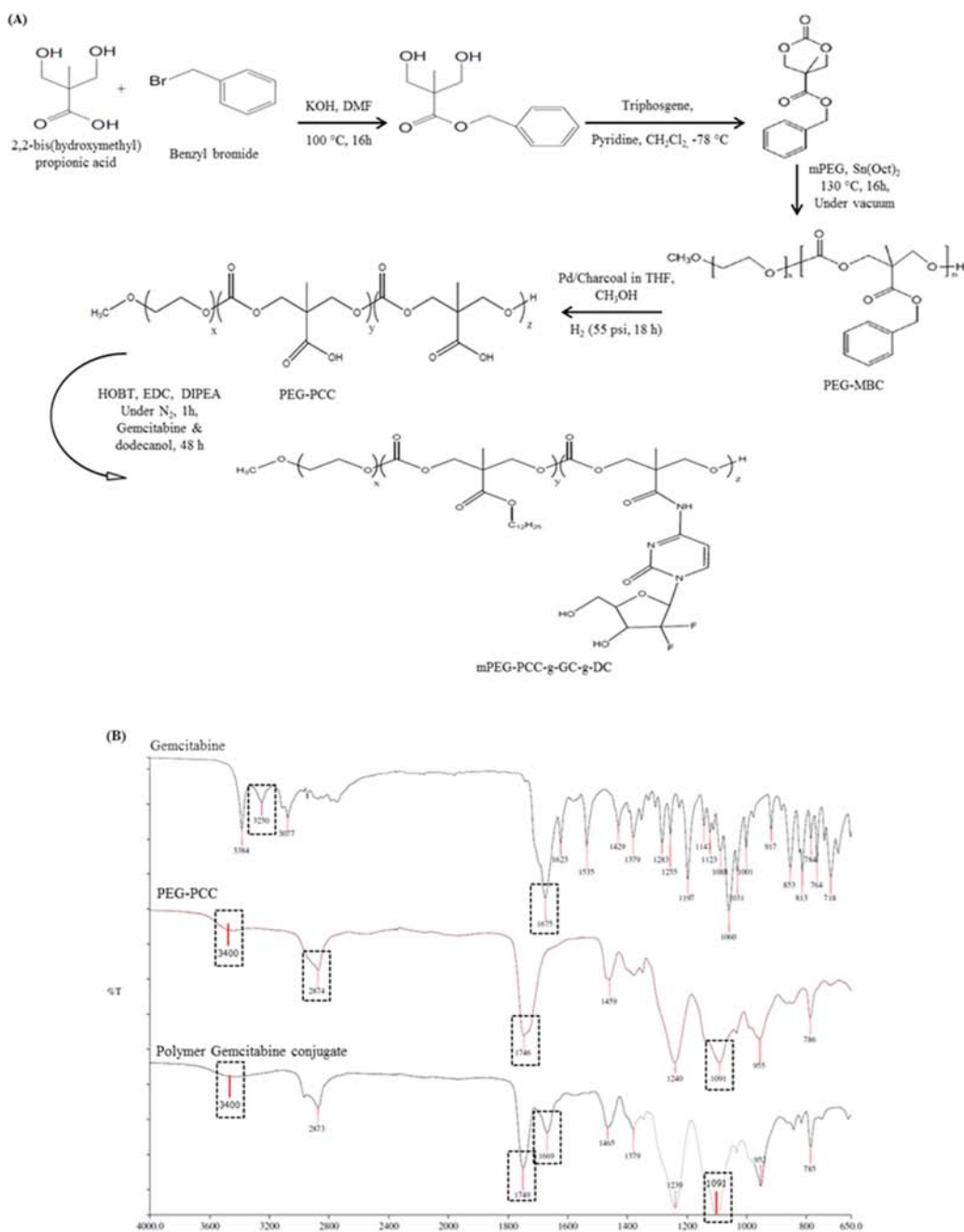


**Figure 1.** Gemcitabine conjugated amphiphilic polymer. (A) Synthesis scheme. (B) FTIR spectral analysis.

inhibit cytidine deaminase enzyme and 20  $\mu\text{L}$  of 2'-deoxy cytidine) was added as an internal standard. Gemcitabine and its metabolite (dFdU) were extracted from plasma by precipitation using acetonitrile (500  $\mu\text{L}$ ) followed by centrifugation at 5000 rpm for 5 min. The supernatant was taken and analyzed using LC-MS method. Chromatographic separation was performed on XterraMS C18 column (2.5  $\mu\text{m}$ , 4.6 mm  $\times$  50 mm) with acetonitrile:water (containing 0.1% formic acid) (20:80) as the mobile phase run at a flow rate of 0.35 mL/min. Injection volume was kept at 20  $\mu\text{L}$ . Calibration curves for gemcitabine and dFdU were plotted in the concentration range of 50–5000 ng/mL.

**In Vitro Cell Culture Studies.** MIA PaCa-2 cells were obtained as a kind gift from Dr. Fazlul H. Sarkar (Wayne State University, Detroit, MI) and L3.6pl cells were purchased from ATCC (Manassas, VA). Both cell lines were maintained in Dulbecco's

Modified Eagle Medium (DMEM) containing 10% fetal bovine serum and 1% antibiotic in an incubator at 37  $^{\circ}\text{C}$ /5%  $\text{CO}_2$ .

**Cytotoxicity Assay.** For cytotoxicity evaluation, cells (5000/well) were seeded in 96 well culture plates and allowed to attach at 37  $^{\circ}\text{C}$ /5%  $\text{CO}_2$ . After 24 h, culture media was removed and fresh media (200  $\mu\text{L}$ ) containing gemcitabine or polymer drug conjugate micelles were added. Cells were incubated at 37  $^{\circ}\text{C}$ /5%  $\text{CO}_2$  for 72 h followed by assessment of cell viability by MTT assay. The absorbance was measured at 560 nm and corrected for the cell debris by subtracting absorbance at 655 nm. Cell viability was calculated using eq 2. To assess the toxicity of the blank copolymer, cytotoxicity of the copolymer without gemcitabine, i.e., mPEG-*b*-PCC-g-DC, was also assessed using the same protocol in the concentration range of 10  $\mu\text{g}/\text{mL}$  to 1000  $\mu\text{g}/\text{mL}$ .

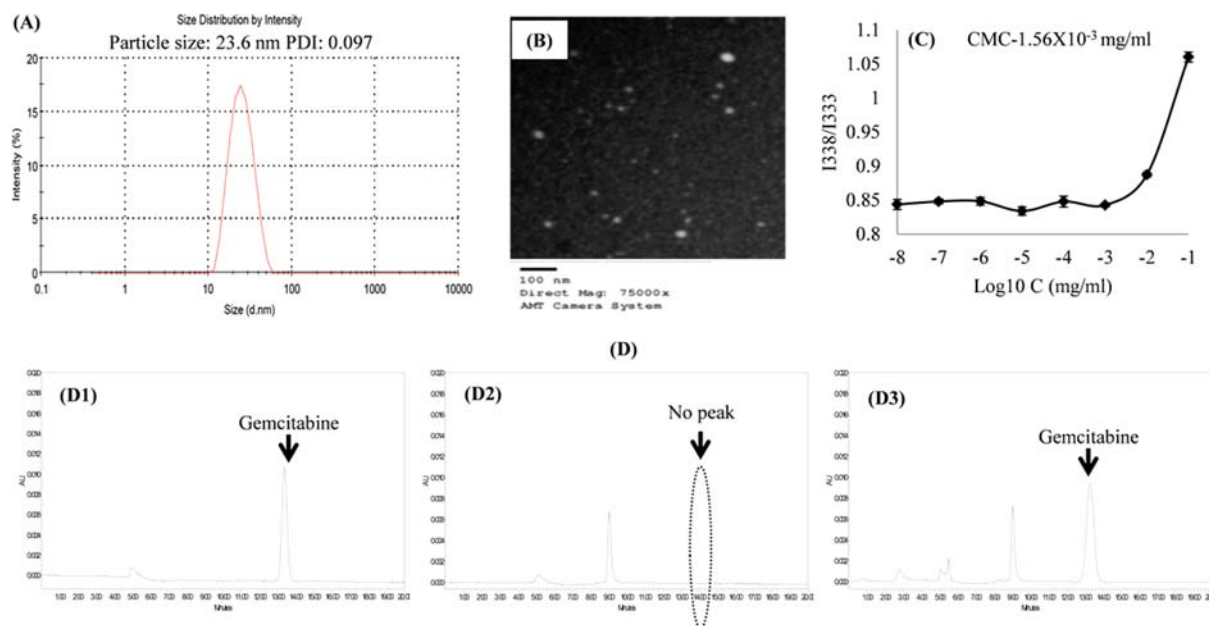


**Figure 2.** Characterization of gemcitabine conjugated polymeric micelles. (A) Particle size analysis. (B) Transmission electron microscopy (TEM) image. (C) Critical micellar concentration (CMC). (D) gemcitabine payload in the formulation analyzed by HPLC. (D1) gemcitabine standard, (D2) and (D3) gemcitabine conjugated polymeric micelles before and after alkaline hydrolysis, respectively. D2 shows that the entire amount of drug is conjugated to the polymer and no free drug is seen.

$$\text{Cell viability(\%)} = \frac{\text{Absorbance of test sample}}{\text{Absorbance of control}} \times 100 \quad (2)$$

**Subcellular Fate of Gemcitabine Polymer Conjugate Micelles.** The intracellular localization of gemcitabine conjugated micelles into the lysosomes and endosomes was determined using LysoTracker Red DND-99 (an acidic organelle dye, Ex/Em 577/590 nm). MIA PaCa-2 cells ( $4 \times 10^4$  cells/well) were plated in a 24-well cell culture plate in 1 mL of media and incubated overnight for attachment. Next day, the cells were treated with free gemcitabine and gemcitabine conjugated micelles at a concentration of 100 nM for 24 and 72 h. The control cells were left untreated. After the predetermined incubation period, the cells were washed with PBS (pH 7.4) and incubated with the media containing LysoTracker Red DND-99 (4  $\mu$ L of 1 mM DMSO solution in 40 mL of media) for 30 min in the dark. Thereafter, the cells were washed thrice with PBS and fixed for 20 min using 10% buffered formaldehyde. The images were observed in Zeiss fluorescent microscope (Axio) using standard Cyt3 filter set at 20 $\times$  magnification to detect the formation of lysosomes.

**Apoptosis Measurement.** The extent of apoptosis induced by free gemcitabine and gemcitabine conjugated micelles in pancreatic cancer cells were studied by TUNEL assay using manufacturer's protocol. Briefly, MIA PaCa-2 cells ( $4 \times 10^4$  cells/well) were plated in chamber slides and incubated overnight for attachment. The cells were then treated with the media containing free gemcitabine and gemcitabine conjugated micelles at a concentration of 100 nM for 72 h while the control cells were left untreated. Thereafter, the cells were fixed using 10% buffered formaldehyde followed by washing twice with PBS. The cells were permeabilized by immersing the slides in 0.2% Triton X-100 solution for 5 min followed by incubation with equilibration buffer (100  $\mu$ L) consisting of 200 mM potassium cacodylate (pH 6.6 at 25  $^{\circ}$ C), 25 mM Tris-HCl (pH 6.6 at 25  $^{\circ}$ C), 0.2 mM DTT, 0.25 mg/mL BSA, and 2.5 mM cobalt chloride, and allowed to equilibrate at room temperature for 10

min. The slides were blotted dry and rTdT incubation buffer (50  $\mu$ L) was added to the cells followed by incubation of the slides at 37  $^{\circ}$ C for 60 min inside the humidified chamber to allow the tailing reaction to occur. The reaction was terminated by immersing the slides in 2 $\times$  saline-sodium citrate buffer (SSC) in a Coplin jar for 15 min at room temperature. Unincorporated fluorescein-12-dUTP was removed by repeated washings with PBS. The samples were counterstained with propidium iodide (1  $\mu$ g/mL) for 15 min at room temperature in the dark followed by washing with PBS. The samples were immediately analyzed under Olympus fluorescence microscope using the standard fluorescein filter set to view the green fluorescence of fluorescein at  $520 \pm 20$  nm and red fluorescence of propidium iodide at  $>620$  nm.

**In Vivo Evaluation in Xenograft Models.** All animal experiments were performed in accordance with the NIH animal use guidelines and protocol approved by the Institutional Animal Care and Use Committee (IACUC) at the University of Tennessee Health Science Center (UTHSC, Memphis, TN). Heterotopic xenograft flank tumors were established in 6–8 week old male NOD.Cg-Prkdcscid Il2rgtm1wj/SzJ (NSG) mice by subcutaneous injection of  $2 \times 10^6$  MIA PaCa-2 pancreatic cancer cells suspended in 1:1 serum-free media and Matrigel (BD Biosciences, CA). When the tumor volume had reached 200 mm<sup>3</sup> animals were randomly divided into three groups with each group containing six animals and samples were administered via tail vein once a week for three weeks. Group 1 was kept as the control and received normal saline, group 2 received free gemcitabine as aqueous solution (40 mg/kg), and group 3 received gemcitabine conjugated polymeric micelles equivalent to free gemcitabine (40 mg/kg). Tumor sizes were measured daily using digital vernier calipers in two perpendicular axis and reported as tumor volume ( $V = 1/2[a \times b^2]$ ,  $a$  = longest axis,  $b$  = shortest axis). Body weight of the animals was recorded every day. At the end of the study (i.e., day 20), tumor tissues were excised and weighed.

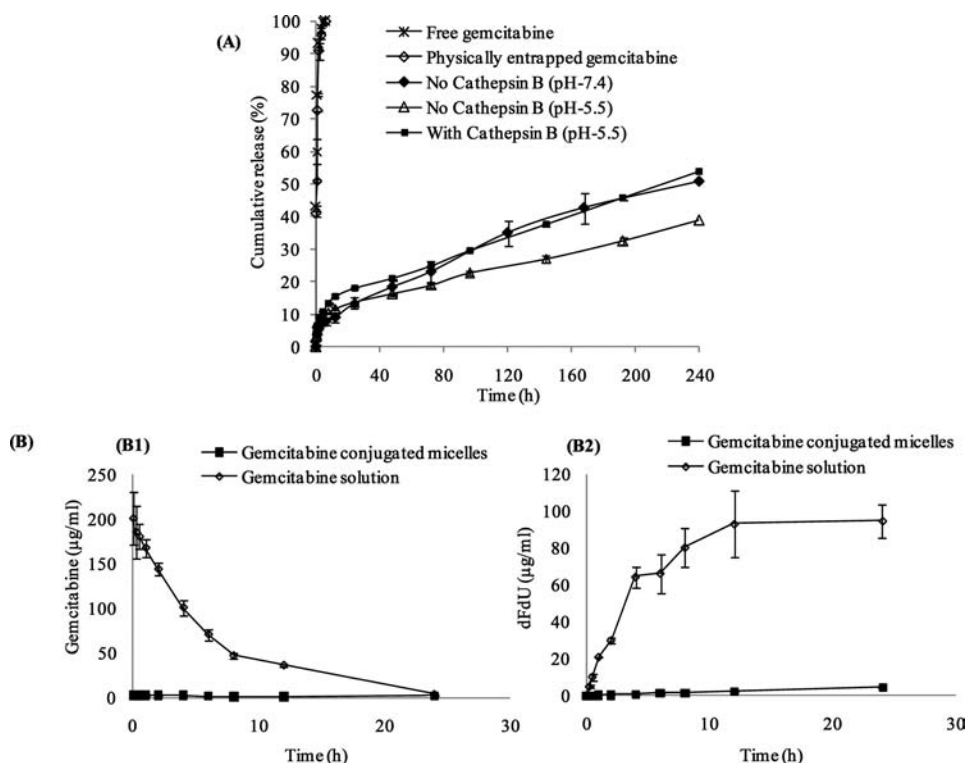


**Figure 3.** Release of gemcitabine from aqueous solution vs methoxy poly(ethylene glycol)-*block*-poly(2-methyl-2-carboxyl-propylenecarbonate-*graft*-gemcitabine-*graft*-dodecanol) polymer drug conjugate micelles after containing equivalent gemcitabine content (A) in PBS at pH 5.5 and 7.4 in the presence and absence of protease Cathepsin B, and (B) in human plasma, (B1) Gemcitabine, and (B2) dFdU.

**Histological Analyses.** At the end of the treatment (i.e., day 20), three representative tumor tissues were harvested per experimental group and fixed with 10% buffered formaldehyde. The fixed tissues were embedded in paraffin and thin sections of 4  $\mu\text{m}$  were obtained. To detect the extent of tumor cell apoptosis, the slides were stained with TUNEL and counterstained with propidium iodide dye (Invitrogen) and visualized under Zeiss fluorescence microscope (Axio).

**Statistical Analysis.** Statistical evaluation was performed by using Student's *t* test. The significance level was set at  $p < 0.05$ .

## RESULTS

**Synthesis and Characterization of Polymer Drug Conjugate.** Polymer drug conjugate was synthesized by direct coupling of gemcitabine onto the free carboxylic acid groups present on the hydrophobic block of the amphiphilic copolymer, PEG-PCC as illustrated in Figure 1A. Gemcitabine and dodecanol were coupled to PEG-PCC using EDC and HOBt coupling chemistry and purified conjugate was characterized by  $^1\text{H}$  NMR and FTIR. In  $^1\text{H}$  NMR spectra of PEG-PCC, protons corresponding to  $-\text{CH}_2-\text{CH}_2-\text{O}-$  of PEG were observed at  $\delta$  3.4–3.6, and  $-\text{CH}_2-$  units of PCC  $\delta$  4.2–4.4 and  $-\text{COOH}$  were observed at  $\delta$  12–14 as reported earlier by our group.<sup>39</sup> Average molecular weight of PEG-PCC was 8680 Da with 23 PCC units as determined using integral value corresponding to protons of  $-\text{CH}_2$  of PEG and  $-\text{CH}_2$  of PCC units. After conjugation of gemcitabine to PEG-PCC, protons corresponding to gemcitabine were observed in the NMR spectra:  $^1\text{H}$  NMR of deuterated dimethyl sulfoxide ( $\text{DMSO}-d_6$ ) of conjugate,  $\delta$  9.6 (s, 1H,  $-\text{NC}(=\text{R})\text{H}$ ), 8.4 (s, 1H,  $-\text{NHCO}-$ ), 6.0–6.2 (m, 1H,  $-\text{CH}$ ), 4.2–4.6 (4nH, proton of PCC  $-\text{CH}_2$ ), 4.0–4.2 (2yH, protons of dodecanol  $-\text{CH}_2-\text{O}$ ), 3.4–3.8 (s, 4mH, Protons of PEG unit

$-\text{CH}_2-\text{CH}_2-\text{O}-$ ), 1–1.5 (m, protons of PCC units  $-\text{CH}_3$  and dodecanol units  $-\text{CH}_2$ ). The FTIR spectra of PEG-PCC shows the characteristic peaks at  $3400\text{ cm}^{-1}$  for stretching vibrations of  $-\text{OH}$  group,  $2874\text{ cm}^{-1}$  for  $-\text{CH}$  stretching vibrations for symmetric and antisymmetric modes of methylene groups,  $1746\text{ cm}^{-1}$  for carbonyl group, and  $1091\text{ cm}^{-1}$  for C–O–C stretching vibration of repeated  $-\text{O}-\text{CH}_2-\text{CH}_2-$  units of PEG (Figure 1B). Gemcitabine shows characteristic peaks for amide bands at  $1675\text{ cm}^{-1}$  and  $3250\text{ cm}^{-1}$  for stretching vibration of  $-\text{NH}_2$ . After conjugation with PEG-PCC, characteristic peaks were obtained at  $3400\text{ cm}^{-1}$  (stretching vibrations of  $-\text{OH}$  group),  $1749\text{ cm}^{-1}$  (for carbonyl group),  $1669\text{ cm}^{-1}$  (amide band), and  $1091\text{ cm}^{-1}$  (for C–O–C stretching vibrations).

**Formulation Development.** Upon nanoprecipitation, gemcitabine conjugated polymer self-assembled into micelles with the mean particle size of  $23.6 \pm 4\text{ nm}$  and PDI of 0.097 as observed by dynamic light scattering. This indicates the formation of a nanosized formulation with a highly homogeneous particle size distribution. TEM images of the formulation revealed the formation of spherical micelles (Figure 2A and B). CMC is an important determinant to evaluate the micelle forming ability of the gemcitabine conjugated copolymer. CMC determined by fluorescence spectroscopy using pyrene as the probe was  $1.56 \times 10^{-3}\text{ mg/mL}$  (Figure 2C). HPLC-UV analysis after alkaline hydrolysis of gemcitabine conjugated micelles showed a peak at 13.25 min corresponding to gemcitabine (Figure 2D3). Further, free gemcitabine was stable under alkaline hydrolysis conditions. A gemcitabine payload of 12.8% w/w was found in the micelles.

**In Vitro Gemcitabine Release Studies.** *In vitro* release studies carried out in PBS (pH 5.5) showed a controlled release of gemcitabine from the micelles, which remained sustained even in the presence of proteolytic enzyme Cathepsin B. The presence

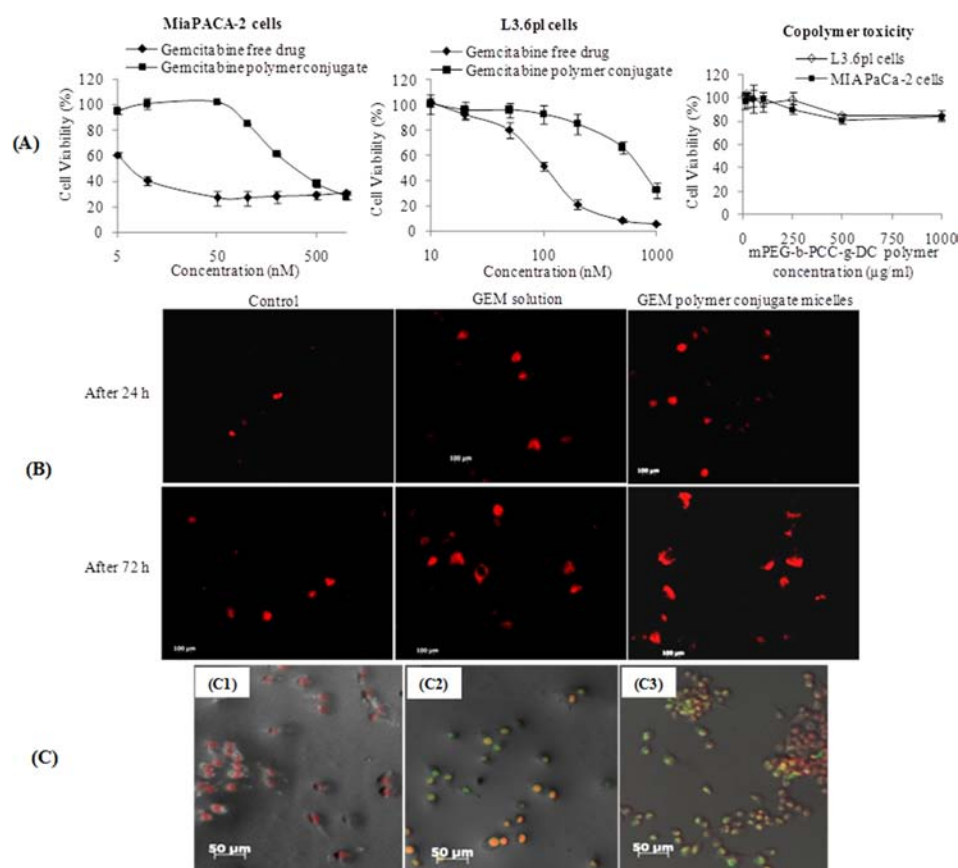


**Figure 4.** Efficacy of gemcitabine conjugated micelles in pancreatic cancer cell lines. (A) Cytotoxicity profiles in MIA PaCa-2 and L3.6pl after 72 h of treatment. (B) Intracellular fate of gemcitabine conjugated micelles shown by staining with LysoTracker Red DND-99 after 24 and 72 h of treatment. Magnification: 20 $\times$ . (C) Apoptosis measurement in MIA PaCa-2 using TUNEL staining. The image shows cells after treatment with (C1) Control, (C2) free gemcitabine as aqueous solution, and (C3) gemcitabine conjugated micelles. Images show the overlay of bright field, PI (red for cell nucleus) and TUNEL staining (green for apoptosis). Magnification: 10 $\times$ .

of enzyme in the release media increased the rate of drug release. The difference in release was less visible initially as 9.08% was released with enzyme while 6.80% was released without enzyme in the first 2 h. However, this difference became more pronounced with time, since 13.67% and 39% release was observed on days 1 and 10, respectively in the absence of the enzyme, while under the influence of enzyme, 18.05% and 53.89% gemcitabine was released on days 1 and 10, respectively (Figure 3A). The rate of gemcitabine release from the conjugated micelles was higher at pH 7.4 compared to pH 5.5. To assess the ability of micelles to physically entrap and control the release of gemcitabine, the dialysis bag method was used similar to that of gemcitabine conjugated micelles. Gemcitabine solution was kept as a control for assessing the hindrance caused by dialysis membrane to the diffusion of free drug to the external media. It was observed that entire gemcitabine was diffused out within 4 h and there was no difference in the diffusion of free gemcitabine and physically entrapped gemcitabine indicating the inability of micelles to physically entrap and control the release of gemcitabine (Figure 3A). This was expected since gemcitabine is a hydrophilic molecule and has a high tendency to remain in the outer aqueous phase and not in the core of the micelles, which is hydrophobic.

**Plasma Stability.** Stability of micelles in plasma was studied by determining the amount of intact gemcitabine released from the formulation and its metabolite dFdU formed after incubation in human plasma. LC-MS method was used to determine

gemcitabine and dFdU concentrations which gave peaks at retention times of 4.3 and 7.2 min, respectively, while retention time of internal standard was obtained at 3.5 min. Free gemcitabine on incubation with plasma showed a drastic reduction in its concentration from 200  $\mu\text{g}/\text{mL}$  to 3  $\mu\text{g}/\text{mL}$  while the concentration of its metabolite dFdU was increased from 0 to 95  $\mu\text{g}/\text{mL}$  within 24 h. However, in the case of gemcitabine conjugated polymeric micelles, only 3  $\mu\text{g}/\text{mL}$  of intact gemcitabine was detected in plasma and 4.5  $\mu\text{g}/\text{mL}$  of dFdU in 24 h (Figure 3B). Further, plasma samples at 24 h were hydrolyzed by alkaline degradation and analyzed by LC-MS method and conjugated gemcitabine was recovered indicating that the conjugated gemcitabine did not metabolize or change in the conjugate.

**In Vitro Cytotoxicity Assay.** Cytotoxic activity of gemcitabine after conjugating to the amphiphilic copolymer was evaluated by incubating MIA PaCa-2 and L3.6pl pancreatic cells with free gemcitabine or gemcitabine conjugated micelles for 72 h and determining the cell viability using MTT assay. The formulations were found to be cytotoxic against both MIA PaCa-2 and L3.6pl cells with  $\text{IC}_{50}$  values of 149.3 and 741.2 nM, respectively, while free gemcitabine showed  $\text{IC}_{50}$  values of 7.6 and 105.9 nM, respectively. We have also determined the toxicity of the blank polymer, i.e., mPEG-*b*-PCC-g-DC (without gemcitabine) on MIA PaCa-2 and L3.6pl cells and these polymers were found to be nontoxic (Figure 4A).

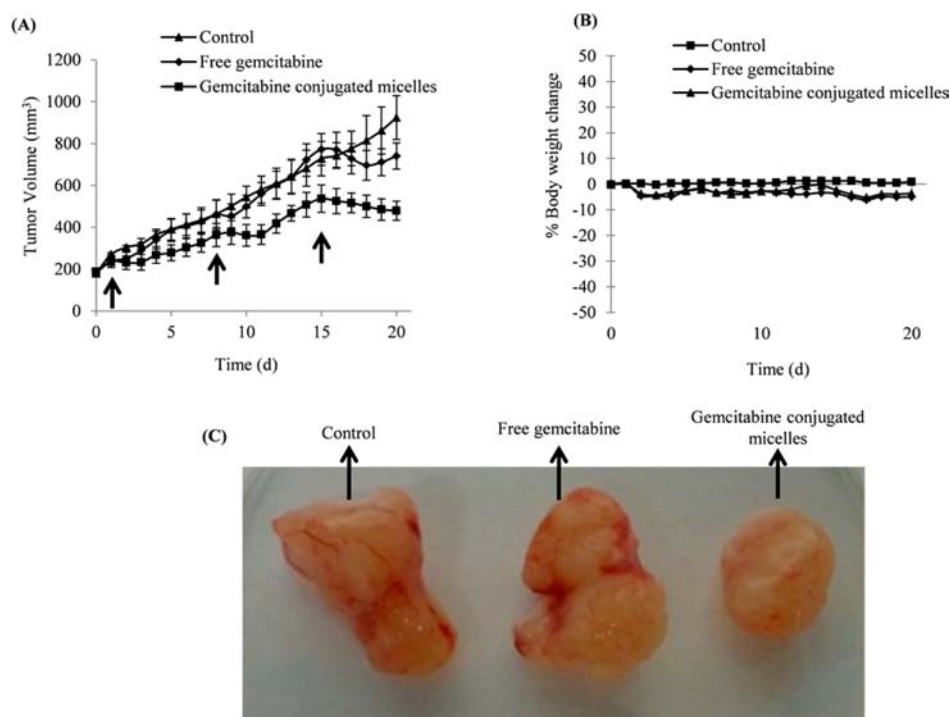


**Figure 5.** *In vivo* efficacy of gemcitabine polymer conjugate in MIA PaCa-2 derived xenograft tumors in NSG mice. Tumors were developed by subcutaneous injection of  $2 \times 10^6$  cells in NSG mice. When tumor size reached  $200 \text{ mm}^3$  animals were treated with gemcitabine or gemcitabine conjugated micellar at a dose of  $40 \text{ mg/kg}$  once weekly for three weeks via intravenous injection through tail vein (indicated by arrow). (A) Change in tumor volume. (B) Change in body weight. (C) Images of tumors excised. Data represented as the mean  $\pm$  SE ( $N = 6$ ).

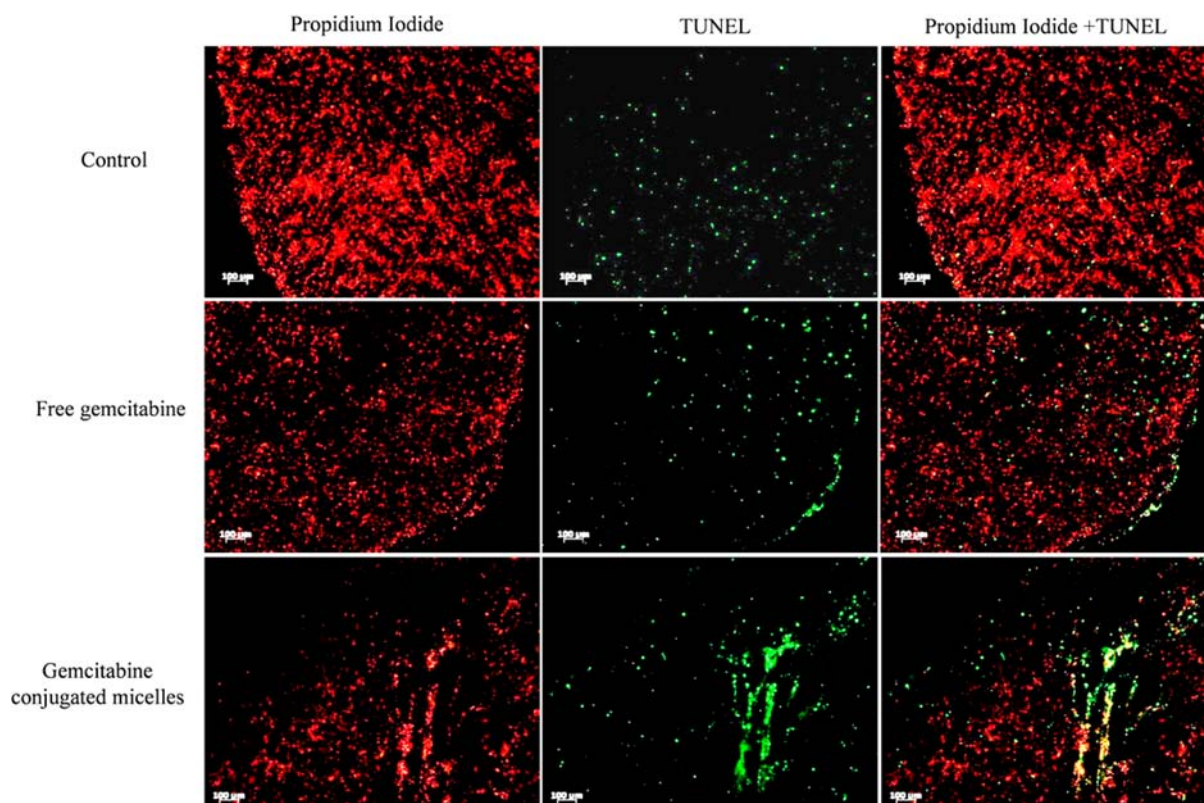


**Figure 6.** Detection of apoptosis induced in the tumor tissues by gemcitabine conjugated micelles in comparison to free drug and control as indicated by the green fluorescence of TUNEL. Red spots mark the cells after staining with propidium iodide. Tissues were excised from the animals at the end of the study, i.e., day 20.



**Intracellular Fate.** Subcellular fate of gemcitabine conjugated polymeric micelles compared to free gemcitabine was studied using LysoTracker Red DND-99 which primarily concentrates in the acidic organelles of the cells. Figure 4B shows the comparative formation of lysosomes and endosomes after treatment of cells with free and conjugated gemcitabine for 24 and 72 h. The control (untreated cells) exhibited few red spots indicating the presence of basal level of lysosomes in the cells; however, in the case of gemcitabine treated cells significantly enhanced punctate fluorescence colocalized with LysoTracker Red was observed indicating the formation of lysosomes. Significantly higher fluorescence intensity was seen in gemcitabine conjugated polymeric micelle treated cells compared to the cells treated with aqueous solution of gemcitabine after 24 h, and the difference became even more predominant after 72 h of treatment.

**Apoptosis Measurement.** Apoptosis is considered to be the key mechanism underlying chemotherapy induced cell death. Figure 4C shows TUNEL assay images of the MIA PaCa-2 cells after incubation with free gemcitabine or gemcitabine conjugated micelles for 24 h. Cells were counterstained with propidium iodide which showed red fluorescence. No apoptosis was observed in the control cells, while both free gemcitabine and gemcitabine conjugated micelles were able to induce apoptosis in the cells as indicated by the green fluorescence of TUNEL.

**In Vivo Efficacy in Xenograft Model.** Gemcitabine conjugated micelles were tested in MIA PaCa-2 cell derived xenograft model in NSG mice. Animals treated with gemcitabine conjugated micelles showed significantly reduced tumor growth rate as compared to gemcitabine solution or the control group (Figure 5A). Further, it was observed that, after injecting gemcitabine conjugated polymeric micelles, the decrease in tumor volume was maintained for at least 4 days before again showing an increase in contrast to gemcitabine solution wherein tumor volume exhibited a continuously increasing pattern until the last injection, and no significant difference was observed between animals treated with free gemcitabine and the control group (untreated). Figure 5B shows the change in body weight of the animals, which was less than 5% for both free gemcitabine and gemcitabine conjugated micelles indicating tolerance of doses given to animals. At the end of the study tumors were excised, weighed, and photographed (Figure 5C) which clearly showed significant difference in the tumor weights of groups treated with gemcitabine conjugated micelles compared to free gemcitabine or the control group (0.38 g versus 0.58 g). The extent of apoptosis in the tumor tissues as indicated by TUNEL assay (Figure 6) was also in agreement with these results, since not much difference was observed between free gemcitabine treated and the control group, while the group treated with gemcitabine conjugated polymeric micelles induced a significantly higher apoptosis which might be responsible for a better antitumor activity of the conjugate compared to the free drug.

## DISCUSSION

A viable strategy for treating pancreatic ductal adenocarcinoma is the need of the hour due to its growing prevalence and high mortality rate. Surgery, radiation, and chemotherapy constitute the major treatment modalities; however, each suffers its own specific limitations mainly arising from local recurrence and metastatic spread of the disease. Chemoresistance in pancreatic cancer results from the desmoplastic tumor microenvironment which inhibits the infiltration of anticancer drugs, particularly hydrophilic molecules like gemcitabine. Extensive research

efforts are being made to devise an effective delivery system for gemcitabine considering its high chemotherapeutic potential for treating pancreatic cancer, which is, however, not yet completely realized clinically owing to its poor pharmacokinetics, rapid plasma metabolism, and extremely high hydrophilicity. Bioconjugation to a polymeric carrier provides an attractive strategy to deliver gemcitabine to the tumor tissue after systemic administration protecting it from plasma metabolism and passively delivering the drug to the tumor compartment. In line with this approach, several lipidic conjugates,<sup>26,28</sup> squalenoyl derivatives,<sup>20,21,23</sup> and PEGylated conjugates of gemcitabine<sup>29</sup> have been prepared and explored for enhanced anticancer properties. However, these systems were limited by poor solubility, uptake by the RES, and/or lower gemcitabine payload.

In the present study, we synthesized a self-assembling, amphiphilic copolymer PEG-PCC with several carboxyl pendant groups on the hydrophobic block and conjugated gemcitabine to these carboxyl groups via EDC/HOBT coupling. The presence of PEG ensures the stealth properties of gemcitabine conjugated micelles, while the presence of carboxyl groups enable the conjugation of higher content of gemcitabine to the polymer resulting in higher payload compared to previously reported PEG conjugates.<sup>5,6</sup> Additionally, we also attached a lipid, dodecanol, to impart requisite hydrophobicity and thus assist in self-assembly and micellization to a very small size (~23 nm) compared to other nanocarrier systems of gemcitabine, thus further ensuring its reduced RES uptake. PEG-PCC copolymer showed poor solubility in organic solvents such as chloroform, acetone, and dichloromethane, but was soluble in THF and DMSO. After conjugation of gemcitabine and dodecanol to the PCC block, its solubility showed marked increase in acetone, CHCl<sub>3</sub>, and CH<sub>2</sub>Cl<sub>2</sub>. <sup>1</sup>H NMR and FTIR confirmed the conjugation of gemcitabine to the copolymer. Gemcitabine content determined by HPLC-UV assay showed a drug loading of 12.8% and also indicated absence of any unconjugated drug (Figure 2D2). This could be attributed to the presence of several carboxylic groups in the hydrophobic PCC segment of copolymer PEG-PCC for conjugation with gemcitabine thus ensuring an appreciable loading of the drug which is otherwise difficult to obtain in the case of hydrophilic drugs. Previously reported PEGylated derivatives of gemcitabine have shown a comparatively poor loading of the drug ranging from 0.98% to 6.79% w/w.<sup>5,6</sup> In this study, gemcitabine conjugated polymer self-assembled into nanosized micelles of 23.6 nm (Figure 2A) indicating their ability to escape from the RES system and extravasate into the tumor compartment. Although our formulation needs improvement in terms of payload compared to gemcitabine-squalene nanoassemblies which showed a payload of 41% w/w,<sup>21,23,24</sup> these gemcitabine conjugated micelles offer several additional advantages over the squalenoylated nanoassemblies. These micelles showed a much smaller micellar size as compared to gemcitabine-squalene nanoassemblies (23 nm vs 140 nm). Further, PEG outer shell can provide stealth effect to gemcitabine conjugated micelles. In contrast, gemcitabine-squalene nanoassemblies were rapidly removed from the bloodstream by the reticulo-endothelial system (RES),<sup>22</sup> thus requiring PEG coating to reduce opsonization and blood clearance.<sup>29</sup> PEGylation was achieved in squalenoylated gemcitabine nanoassemblies by addition of PEG-squalene or PEG-cholesterol in the weight ratio of 1:0.7 to form composite nanoassemblies. Though addition of PEG-squalene in the formulation resulted in decrease in effective gemcitabine loading in the composite nanoassemblies, however, the

significance of PEG cannot be overruled since the PEGylated gemcitabine nanoassemblies showed improved efficacy over the non-PEGylated nanoassemblies.<sup>29</sup> The presented formulation exhibits a balance between a moderate drug loading (12.8% w/w) and PEG content (~55%).

Since gemcitabine conjugated micelles are intended for intravenous route of administration, it is important that the formulation remains stable and does not release the drug in the plasma which would otherwise undergo plasma metabolism and would not reach therapeutically effective levels in the tumor tissue. Once in the systemic circulation, the effect of blood dilution on the stability of micellar formulation could be alleviated by designing polymers which show a low CMC value, which in the present case was 1.56  $\mu\text{g}/\text{mL}$ . This CMC value is much lower than reported with frequently used nonionic surfactants, Tween 80 and Tween 20 (both  $\sim 300 \mu\text{g}/\text{mL}$ ),<sup>40</sup> Pluronic block copolymers ( $\sim 25\text{--}299 \mu\text{g}/\text{mL}$ ),<sup>41</sup> or with other synthetic PEG based amphiphilic polymers designed to deliver gemcitabine as micelles ( $\sim 4 \mu\text{g}/\text{mL}$  and  $\sim 70 \mu\text{g}/\text{mL}$ ),<sup>33,42,43</sup> and thus the formulation is expected to be stable against dilution. Chemically, gemcitabine is a stable molecule;<sup>44</sup> however, on intravenous administration it undergoes rapid metabolism by cytidine deaminase enzyme to its inactive metabolite, dFdU. Thus, one objective of the work was to improve the *in vivo* stability toward metabolism in plasma and hence to enhance its delivery *in vivo*. Upon incubation with human plasma, gemcitabine conjugated micelles still retained more than 98% of the drug for 24 h (Figure 3B) indicating that attaching the polymer at N4 of gemcitabine imparted protection to the drug from plasma deamination. This shows a significant improvement over the previous attempts to curtail drug metabolism whereby PEGylated and linoleic acid based conjugates of gemcitabine, when incubated in plasma, still exhibited 30–40% of drug release within 24 h.<sup>5,25</sup> This could be attributed to the presence of conjugated gemcitabine inside the core of the micelles thereby decreasing its accessibility to the enzyme activity and/or hydrolysis and ensuring a sustained and targeted release of the drug. Polymer drug conjugates are taken up by the cells via endocytosis, and once inside the cells, these must be internalized by the lysosomes and endosomes so as to ensure the degradation of the conjugate to facilitate the release of active moiety and exhibit its resultant therapeutic benefit.<sup>6</sup> Incubation of MIA PaCa-2 pancreatic cells with the conjugate for 24 h showed higher fluorescence intensity, signifying enhanced formation of lysosomes and endosomes inside the cells and better internalization of gemcitabine via drug polymer conjugate vs free drug (Figure 4B). Increase in the fluorescence intensity after 72 h also indicates the elevated retention of gemcitabine via conjugated micelles with time. PEGylated gemcitabine conjugates reported by Sahoo et al. also showed similar behavior and were retained inside the lysosomes for a longer duration of time.<sup>6</sup> Once inside, the conjugate shall be degraded inside the acidic and enzyme-rich environment of these organelles and thus enable release of gemcitabine. To confirm the liberation of the free drug from the conjugate, drug dissociation from the polymer conjugate was studied in the presence and absence of cathepsin B (a cysteine protease) at acidic pH 5.5 (to mimic the lysosomal compartment). Previous studies have shown that gemcitabine remains stable under these conditions.<sup>16</sup> We observed that 54% of the total conjugated drug was released from the conjugate in 10 days while 39% release was observed in absence of Cathepsin B. Further, the release at pH 7.4 was faster than at pH 5.5 with 50.8% release in 10 days. The results indicate that the drug

release is not entirely dependent on the enzymatic activity but is enhanced in its presence. However, the linkage of drug to polymer may break *in vitro* without enzyme being present in the media by hydrolysis leading to the release of gemcitabine. Further, it was evident from this data that the drug could dissociate itself from the polymer drug conjugate in an acidic and enzyme-rich environment to elicit its therapeutic action, along with the ability of the synthesized conjugate to sustain and control the release of gemcitabine, which is otherwise a challenge in the case of hydrophilic drugs. Cathepsin B is a lysosomal protease which can enzymatically cleave the amide bonds between the drug and the polymer and thereby release the drug from the system. Previous reports on polymeric conjugates and prodrugs of gemcitabine have also shown the role of cathepsins in degradation of the amide bond and release of the drug moiety.<sup>20,45,46</sup> We have not tested the mechanism on how cathepsin B will interact with the micelles and result in subsequent drug release. For cathepsin B to act on the linkage of drug and polymer, the micelles should get dissociated. Since micelles exist in a dynamic equilibrium with the molecularly dissolved copolymer molecules (unimers) in the solution, it is expected that the enzyme may act on dissociated copolymer leading to release the drug. Furthermore, the polymer backbone contains the degradable carbonate bonds in the hydrophobic segment of the copolymer, which can undergo hydrolysis in water, liberating the gemcitabine conjugated oligomers or monomers which could be further acted upon by enzyme resulting in the release of free gemcitabine. Other polymeric conjugates and lipidic derivatives of gemcitabine, which aimed to prolong the release of this hydrophilic molecule, exhibited as much as 40–50% of the drug release within the initial 48 h,<sup>5,6</sup> but in the present study, the release was much sustained since more than 40% of the drug still remained in the micelles even after 10 days. A possible explanation for slow release could be strong affinity between the conjugated drug and the hydrophobic core of the micelles as also stated by Rijcken et al.<sup>47</sup> The presence of dodecanol in the synthesized polymer could also have imparted additional stability to the system, since lipids have a tendency to stabilize the micellar structures. It is also well-recognized that fatty acid chains stabilize and hold together the phospholipid bilayers of the cell membrane by a variety of forces such as van der Waals interactions.<sup>33</sup> Thus, our conjugate holds a better potential to reduce the dosing frequency and overall dose of gemcitabine and hence moderate the systemic adverse effects and enhance patient compliance over the previously reported gemcitabine conjugates.

The amount and rate of drug release from the conjugate has direct influence on the therapeutic efficacy of the drug. MTT assay indicated that the bioconjugation with the amphiphilic copolymer did not compromise its cytotoxic activity (Figure 4A). Free gemcitabine showed lower  $\text{IC}_{50}$  values, which is in agreement with the previous reports for PEG–gemcitabine conjugates.<sup>5</sup> This difference mainly arises due to the slower uptake of the conjugate which enters the cells via the endocytosis pathway and, second, gemcitabine has to be dissociated from the conjugate inside the cells before showing its activity. Since the polymer is biodegradable and byproducts can form during the hydrolysis of the polymer backbone, we have tested the toxicity of the blank polymer (mPEG-*b*-PCC-g-DC) to confirm any nonspecific toxicity. Results indicated that the polymer and its byproducts were nontoxic to the cells; thus, the cell killing observed in the cytotoxicity assays was due to the gemcitabine. Another confirmation of the preserved therapeutic efficacy of the

drug was observed by carrying out the TUNEL assay which specifically marks the apoptotic cells within a cell population. Similar to free gemcitabine, these conjugates were also able to induce significant apoptosis in the pancreatic cancer cells (Figure 4C). Recently, Maksimenko et al. reported much higher  $IC_{50}$  values in 4 different cancer cell lines and comparable/slightly less apoptotic fractions in MIA PaCa-2 cells upon treatment with isoprenoyl conjugates of gemcitabine compared to the free drug.<sup>48</sup> The evidence of a clear therapeutic benefit which a nanoformulation could yield over free drug is difficult to observe in *in vitro* cell culture studies due to the lack of the biological dynamism and absence of barriers that a drug has to bypass before reaching its target tissue *in vivo*. On the contrary, in the case of cell culture studies, the drug immediately gets into direct contact with the cells which diminishes the advantages offered by nanocarriers in terms of protecting the drug from the hostile GI environment, a different uptake mechanism via Peyer's patches, and thus ensuring a higher absorption and exploiting the EPR effect. To understand if gemcitabine conjugated polymeric micelles offered any therapeutic advantages over the free drug, we carried out the *in vivo* evaluation in xenograft model of pancreatic cancer in NSG mice after intravenous injection (equivalent to 40 mg/kg of gemcitabine). Gemcitabine is usually administered in mice via intraperitoneal route and intravenous route at a dose ranging widely from 7 mg/kg to 500 mg/kg.<sup>23,31,48–51</sup> In the present study, intravenous route was used for free gemcitabine since we wanted to compare the results with the conjugated micelles that were also administered by intravenous route. We have selected a dose of 40 mg/kg based on a previous report for polymer–gemcitabine conjugate,<sup>31</sup> even though this dose is not the maximal tolerable dose (MTD). Compared to free gemcitabine, gemcitabine conjugated micelles efficiently decreased the tumor growth and final tumor weight when administered at the same equivalent dose (Figure 5). This could be attributed to the decreased plasma metabolism of the conjugated gemcitabine owing to blockage of the site of deamination and hindrance provided by the polymeric carrier to the cytidine deaminase enzyme. These results are in agreement with the previous study wherein gemcitabine conjugates have shown superior antitumor activity over free drug.<sup>5,31,48</sup> Further, the nanosize of the micelles could enable enhanced permeation and retention into the tumor compartment. The outer PEG shell of the micelles could prevent its uptake by the RES system and increase its mean residence time in the central compartment. Gemcitabine conjugated micelles suppress the tumor growth more dramatically right after injection compared to free drug. This could be due to faster release of gemcitabine from the micelles in the highly degradable lysosomal environment of the tumor cells compared to only 53.89% gemcitabine release from the micelles *in vitro* in 10 days. This warrants a thorough investigation of the pharmacokinetic–pharmacodynamic profile of the formulation since it could not be predicted solely from *in vitro* drug release as this may change in *in vivo* conditions (in tumor microenvironment or in tumor cells). The efficacy of gemcitabine conjugated micelles is modest as compared to the previous work reported by Harrison et al.<sup>52</sup> and could be attributed to the dosing schedule and more particularly to the different strain of mice (athymic nude mice versus NSG mice) which can affect the pharmacokinetic properties/metabolism of the system *in vivo*. Further, there is no difference in the control group and free gemcitabine which could be due to the inefficacy of the free drug to reach the tumor compartment at the therapeutic level to show any effect. This is also expected and

has been reported previously wherein free gemcitabine treated group did not show any tumor reduction.<sup>52</sup> The antitumor efficacy of gemcitabine mainly results from its ability to induce apoptosis. High antitumor efficacy of squalenoyl–gemcitabine conjugate against aggressive metastatic leukemia model was mainly attributed to induction of apoptosis by the active triphosphate form of gemcitabine after getting incorporated into the DNA.<sup>5</sup> Herceptin-conjugated gemcitabine chitosan nanoparticles have been shown to exhibit superior antiproliferative activity against pancreatic cancer along with an enhanced S-phase arrest, leading to apoptosis in comparison with free gemcitabine.<sup>53</sup> In the present study also, the underlying apoptosis mechanism for enhanced antitumor activity of the conjugate was investigated by the TUNEL assay conducted on the tumor tissue samples (Figure 6). While free gemcitabine induced negligible apoptosis in the tumor cells, the gemcitabine polymer conjugate treated group showed a significantly high number of apoptotic cells. Further, the conjugate did not cause adverse systemic side effects as indicated by the weight change profile of the animals, where the weight of the experimental animals was almost similar to that in the control group.

## ■ CONCLUSION

Gemcitabine was conjugated to an amphiphilic copolymer PEG-PCC, bearing multiple carboxylic groups, thus ensuring a high payload of the drug. Gemcitabine conjugated polymer self-assembled into nanosized micelles which released the drug in a controlled fashion and provided enhanced stability in human plasma since the drug was conjugated to the hydrophobic core of the micelles thereby making it inaccessible to metabolism and improving its stability. The micelles showed considerable reduction in cell viability of pancreatic cancer cell lines by enhanced internalization and apoptotic cell death. *In vivo* evaluation in pancreatic tumor model demonstrated enhanced antitumor activity of the gemcitabine conjugated micelles compared to free drug without inducing any significant toxicity. This might be attributed to the apoptotic cell death induced by micelles in addition to the presence of outer PEG shell which would have provided long circulation and enhanced permeation and retention in the tumor compartment. The system needs to be further evaluated for *in vivo* pharmacokinetics and biodistribution to confirm this fact. In a nutshell, the system offers potential for additional advantages such as loading of another hydrophobic drug in the core for combination therapy and modification of the hydrophobic block by attaching different ligands viz. cationic chains for miRNA delivery. The strategy outlined in this work not only provides a promising approach to be developed as an alternative therapy for an effective pancreatic cancer treatment, but could also be explored for delivery of other difficult-to-deliver hydrophilic drug molecules particularly which have shown high therapeutic potential but modest clinical benefit due to delivery challenges associated with them.

## ■ AUTHOR INFORMATION

### Corresponding Author

\*Tel: 402-559-5422; Fax: 402-559-9543; E-mail: ram.mahato@unmc.edu; Skype: ram.mahato.

### Notes

The authors declare no competing financial interest.

## ACKNOWLEDGMENTS

Kosten foundation is duly acknowledged for providing financial support.

## ABBREVIATIONS

CMC, critical micelle concentration; dFdU, 2',2'-difluorodeoxyuridine; EDC, 1-(3-dimethylaminopropyl)-3-ethylcarbodiimide HCl; HOBT, 1-hydroxybenzotriazole; MBC, 2-methyl-2-benzoyloxycarbonyl-propylene carbonate; mPEG, methoxy polyethylene glycol; PBS, phosphate buffered saline; PDI, polydispersity index; PEG-PCC, poly(ethylene glycol)-*block*-poly(2-methyl-2-carboxyl-propylene carbonate); TEM, transmission electron microscopy; TUNEL, terminal deoxynucleotidyl transferase biotin-dUTP nick end labeling

## REFERENCES

- (1) Giovannetti, E., Funel, N., Peters, G. J., Del Chiaro, M., Erozcenci, L. A., Vasile, E., Leon, L., Pollina, L., Groen, A., Falcone, A., Danesi, R., Campani, D., Verheul, H. M., and Boggi, U. (2010) MicroRNA-21 in pancreatic cancer: correlation with clinical outcome and pharmacologic aspects underlying its role in the modulation of gemcitabine activity. *Cancer Res.* 70, 4528–38.
- (2) Ji, Q., Hao, X., Zhang, M., Tang, W., Yang, M., Li, L., Xiang, D., Desano, J. T., Bommer, G. T., Fan, D., Fearon, E. R., Lawrence, T. S., and Xu, L. (2009) MicroRNA miR-34 inhibits human pancreatic cancer tumor-initiating cells. *PLoS One* 4, e6816.
- (3) Singh, A., and Settleman, J. (2010) EMT, cancer stem cells and drug resistance: an emerging axis of evil in the war on cancer. *Oncogene* 29, 4741–51.
- (4) Wang, Z., Li, Y., Ahmad, A., Banerjee, S., Azmi, A. S., Kong, D., and Sarkar, F. H. (2011) Pancreatic cancer: understanding and overcoming chemoresistance. *Nat. Rev. Gastroenterol. Hepatol.* 8, 27–33.
- (5) Pasut, G., Canal, F., Via, L. D., Arpicco, S., Veronese, F. M., and Schiavon, O. (2008) Antitumoral activity of PEG–gemcitabine prodrugs targeted by folic acid. *J. Controlled Release* 127, 239–48.
- (6) Vandana, M., and Sahoo, S. K. (2010) Long circulation and cytotoxicity of PEGylated gemcitabine and its potential for the treatment of pancreatic cancer. *Biomaterials* 31, 9340–56.
- (7) Reddy, L. H., and Couvreur, P. (2008) Novel approaches to deliver gemcitabine to cancer. *Curr. Pharm. Des.* 14, 1124–37.
- (8) Bormann, C., Graeser, R., Esser, N., Ziroli, V., Jantschke, P., and Keck, T. (2008) A new liposomal formulation of gemcitabine is active in an orthotopic mouse model of pancreatic cancer assessible to bioluminescence imaging. *Cancer Chemother. Pharmacol.* 61, 395–405.
- (9) Calvagno, M. G., Celia, C., Paolino, D., Cosco, D., Iannone, M., Castelli, F., Doldo, P., and Fresta, M. (2007) Effects of lipid composition and preparation conditions on physical-chemical properties, technological parameters and in vitro biological activity of gemcitabine-loaded liposomes. *Curr. Drug Delivery* 4, 89–101.
- (10) Celano, M., Calvagno, M. G., Bulotta, S., Paolino, D., and Arturi, F. (2004) Cytotoxic effects of gemcitabine-loaded liposomes in human anaplastic thyroid carcinoma cells. *BMC Cancer* 4, 63–70.
- (11) Celia, C., Malara, N., Terracciano, R., Cosco, D., Paolino, D., Fresta, M., and Savino, R. (2008) Liposomal delivery improves the growth-inhibitory and apoptotic activity of low doses of gemcitabine in multiple myeloma cancer cells. *Nanomedicine* 4, 155–66.
- (12) Gang, J., Park, S.-B., Hyung, W., Choi, E. H., Wen, J., Kim, H., Shul, Y., Haam, S., and Song, S. Y. (2007) Magnetic poly caprolactone nanoparticles containing Fe<sub>3</sub>O<sub>4</sub> and gemcitabine enhance anti-tumor effect in pancreatic cancer xenograft mouse model. *J. Drug Targeting* 15, 445–53.
- (13) Li, J.-m., Chen, W., Wang, H., Jin, C., Yu, X.-j., Lu, W.-y., Cui, L., Fu, D.-l., Ni, Q.-x., and Hou, H.-m. (2009) Preparation of albumin nanospheres loaded with gemcitabine and their cytotoxicity against BXP-3 cells in vitro. *Acta Pharmacol. Sin.* 30, 1337–43.
- (14) Yang, J., Lee, H., Hyung, W., Park, S.-B., and Haam, S. (2006) Magnetic PECA nanoparticles as drug carriers for targeted delivery: Synthesis and release characteristics. *J. Microencap.* 23, 203–12.
- (15) Yang, J., Park, S.-B., Yoon, H.-G., Huh, Y.-M., and Haam, S. (2006) Preparation of poly caprolactone nanoparticles containing magnetite for magnetic drug carrier. *Int. J. Pharm.* 324, 185–90.
- (16) Kiew, L. V., Cheong, S. K., Sidik, K., and Chung, L. Y. (2010) Improved plasma stability and sustained release profile of gemcitabine via polypeptide conjugation. *Int. J. Pharm.* 391, 212–20.
- (17) Cavallaro, G., Licciardi, M., Salmaso, S., Caliceti, P., and Gaetano, G. (2006) Folate-mediated targeting of polymeric conjugates of gemcitabine. *Int. J. Pharm.* 307, 258–69.
- (18) Moog, R., Burger, A. M., Brandl, M., Schuler, J., Schubert, R., and Unger, C. (2002) Change in pharmacokinetic and pharmacodynamic behavior of gemcitabine in human tumor xenografts upon entrapment in vesicular phospholipid gels. *Cancer Chemother. Pharmacol.* 49, 356–66.
- (19) Ali, S. M., Khan, A. R., Ahmad, M. U., Chen, P., Sheikh, S., and Ahmad, I. (2005) Synthesis and biological evaluation of gemcitabine-lipid conjugate (NEO6002). *Bioorg. Med. Chem. Lett.* 15, 2571–4.
- (20) Couvreur, P., Stella, B., Reddy, L. H., Hillaireau, H., Dubernet, C., Desmaele, D., Lepetre-Mouelhi, S., Rocco, F., Marsaud, V., Renoir, J. M., and Cattel, L. (2006) Squalenoyl nanomedicines as potential therapeutics. *Nano Lett.* 6, 2544–8.
- (21) Reddy, L. H., Dubernet, C., Mouelhi, S. L., Marque, P. E., Desmaele, D., and Couvreur, P. (2007) A new nanomedicine of gemcitabine displays enhanced anticancer activity in sensitive and resistant leukemia types. *J. Controlled Release* 124, 20–7.
- (22) Reddy, L. H., Khoury, H., Paci, A., Deroussent, A., Ferreira, H., Dubernet, C., Declèves, X., Besnard, M., Chacun, H., Lepetre-Mouelhi, S., Desmaele, D., Rousseau, B., Laugier, C., Cintrat, J. C., Vassal, G., and Couvreur, P. (2008) Squalenoylation favorably modifies the in vivo pharmacokinetics and biodistribution of gemcitabine in mice. *Drug Metab. Dispos.* 36, 1570–7.
- (23) Reddy, L. H., Renoir, J. M., Marsaud, V., Lepetre-Mouelhi, S., Desmaele, D., and Couvreur, P. (2009) Anticancer efficacy of squalenoyl gemcitabine nanomedicine on 60 human tumor cell panel and on experimental tumor. *Mol. Pharmaceutics* 6, 1526–35.
- (24) Rejiba, S., Reddy, L. H., Bigand, C., Parmentier, C., Couvreur, P., and Hajri, A. (2011) Squalenoyl gemcitabine nanomedicine overcomes the low efficacy of gemcitabine therapy in pancreatic cancer. *Nanomedicine* 7, 841–9.
- (25) Tao, X. M., Wang, J. C., Wang, J. B., Feng, Q., Gao, S. Y., Zhang, L. R., and Zhang, Q. (2012) Enhanced anticancer activity of gemcitabine coupling with conjugated linoleic acid against human breast cancer in vitro and in vivo. *Eur. J. Pharm. Biopharm.* 82, 401–9.
- (26) Brusa, P., Immordino, M. L., Rocco, F., and Cattel, L. (2007) Antitumor activity and pharmacokinetics of liposomes containing lipophilic gemcitabine prodrugs. *Anticancer Res.* 27, 195–9.
- (27) Pili, B., Reddy, L. H., Bourgaux, C., Lepetre-Mouelhi, S., Desmaele, D., and Couvreur, P. (2010) Liposomal squalenoyl-gemcitabine: formulation, characterization and anticancer activity evaluation. *Nanoscale* 2, 1521–6.
- (28) Stella, B., Arpicco, S., Rocco, F., Marsaud, V., Renoir, J.-M., Cattel, L., and Couvreur, P. (2007) Encapsulation of gemcitabine lipophilic derivatives into polycyanoacrylate nanospheres and nanocapsules. *Int. J. Pharm.* 344, 71–7.
- (29) Bekkara-Aounallah, F., Gref, R., Othman, M., Reddy, L. H., Pili, B., Allain, V., Bourgaux, C., Hillaireau, H., Lepetre-Mouelhi, S., Desmaele, D., Nicolas, J., Chafi, N., and Couvreur, P. (2008) Novel PEGylated nanoassemblies made of self-assembled squalenoyl nucleoside analogues. *Adv. Funct. Mater.* 18, 1–11.
- (30) Aryal, S., Hu, C. M., and Zhang, L. (2010) Combinatorial drug conjugation enables nanoparticle dual-drug delivery. *Small* 6, 1442–8.
- (31) Kiew, L. V., Cheong, S. K., Ramli, E., Sidik, K., Lim, T. M., and Chung, L. Y. (2012) Efficacy of a poly-L-glutamic acid-gemcitabine conjugate in tumor-bearing mice. *Drug Dev. Res.* 73, 120–129.
- (32) Yang, J., Luo, K., Pan, H., Kopeckova, P., and Kopecek, J. (2011) Synthesis of biodegradable multiblock copolymers by click coupling of

RAFT-generated heterotelechelic PolyHPMA conjugates. *React. Funct. Polym.* 71, 294–302.

(33) Zhu, S., Lansakara, P. D., Li, X., and Cui, Z. (2012) Lysosomal delivery of a lipophilic gemcitabine prodrug using novel acid-sensitive micelles improved its antitumor activity. *Bioconjugate Chem.* 23, 966–80.

(34) Chitkara, D., Singh, S., Kumar, V., Danquah, M., Behrman, S. W., Kumar, N., and Mahato, R. I. (2012) Micellar delivery of cyclophamide and gefitinib for treating pancreatic cancer. *Mol. Pharm.* 9, 2350–57.

(35) Li, F., Lu, Y., Li, W., Miller, D. D., and Mahato, R. I. (2010) Synthesis, formulation and in vitro evaluation of a novel microtubule destabilizer, SMART-100. *J. Controlled Release* 143, 151–8.

(36) Danquah, M., Fujiwara, T., and Mahato, R. I. (2010) Self-assembling methoxypoly(ethylene glycol)-b-poly(carbonate-co-L-lactide) block copolymers for drug delivery. *Biomaterials* 31, 2358–70.

(37) Wang, X. L., Zhuo, R. X., Liu, L. J., He, F., and Liu, G. (2002) Synthesis and characterization of novel aliphatic polycarbonates. *J. Polym. Sci., Part A: Polym. Chem.* 40, 70–5.

(38) Zhu, K. J., Hendren, R. W., Jensen, K. J., and Pitt, C. G. (1991) Synthesis, properties and biodegradation of poly(1,3-trimethylene carbonate). *Macromolecules* 24, 1736–40.

(39) Li, F., Danquah, M., and Mahato, R. I. (2010) Synthesis and characterization of amphiphilic lipopolymers for micellar drug delivery. *Biomacromolecules* 11, 2610–20.

(40) Lo, Y. L. (2003) Relationships between the hydrophilic lipophilic balance values of pharmaceutical excipients and their multidrug resistance modulating effect in Caco-2 cells and rat intestines. *J. Controlled Release* 90, 37–48.

(41) Kabanov, A. V., Batrakova, E. V., and Miller, D. W. (2003) Pluronic block copolymers as modulators of drug efflux transporter activity in the blood-brain barrier. *Adv. Drug Delivery Rev.* 55, 151–64.

(42) Aryal, S., Hu, C. M., and Zhang, L. (2010) Polymer-cisplatin conjugate nanoparticles for acid-responsive drug delivery. *ACS Nano* 4, 251–8.

(43) Tang, R., Ji, W., Panus, D., Palumbo, R. N., and Wang, C. (2011) Block copolymer micelles with acid-labile ortho ester sidechains: Synthesis, characterization, and enhanced drug delivery to human glioma cells. *J. Controlled Release* 151, 18–27.

(44) Xu, Q., Zhang, Y., and Trissel, L. A. (1999) Physical and chemical stability of gemcitabine hydrochloride solutions. *J. Am. Pharm. Assoc. (Wash.)* 39, 509–13.

(45) Lammers, T., Subr, V., Ulbrich, K., Peschke, P., Huber, P. E., Hennink, W. E., and Storm, G. (2009) Simultaneous delivery of doxorubicin and gemcitabine to tumors in vivo using prototypic polymeric drug carriers. *Biomaterials* 30, 3466–75.

(46) Immordino, M. L., Brusa, P., Rocco, F., Arpicco, S., Ceruti, M., and Cattel, L. (2004) Preparation, characterization, cytotoxicity and pharmacokinetics of liposomes containing lipophilic gemcitabine prodrugs. *J. Controlled Release* 100, 331–46.

(47) Rijcken, C. J., Soga, O., Hennink, W. E., and van Nostrum, C. F. (2007) Triggered destabilisation of polymeric micelles and vesicles by changing polymers polarity: an attractive tool for drug delivery. *J. Controlled Release* 120, 131–48.

(48) Maksimenko, A., Mougin, J., Mura, S., Sliwinski, E., Lepeltier, E., Bourgaux, C., Lepetre, S., Zouhiri, F., Desmaele, D., and Couvreur, P. (2013) Polyisoprenoyl gemcitabine conjugates self assemble as nanoparticles, useful for cancer therapy. *Cancer Lett.* 334, 346–53.

(49) Sun, F. X., Tohgo, A., Bouvet, M., Yagi, S., Nassirpour, R., Moossa, A. R., and Hoffman, R. M. (2003) Efficacy of camptothecin analog DX-8951f (Exatecan Mesylate) on human pancreatic cancer in an orthotopic metastatic model. *Cancer Res.* 63, 80–5.

(50) Bruns, C. J., Shrader, M., Harbison, M. T., Portera, C., Solorzano, C. C., Jauch, K. W., Hicklin, D. J., Radinsky, R., and Ellis, L. M. (2002) Effect of the vascular endothelial growth factor receptor-2 antibody DC101 plus gemcitabine on growth, metastasis and angiogenesis of human pancreatic cancer growing orthotopically in nude mice. *Int. J. Cancer* 102, 101–8.

(51) Bruns, C. J., Harbison, M. T., Davis, D. W., Portera, C. A., Tsan, R., McConkey, D. J., Evans, D. B., Abbruzzese, J. L., Hicklin, D. J., and Radinsky, R. (2000) Epidermal growth factor receptor blockade with

C225 plus gemcitabine results in regression of human pancreatic carcinoma growing orthotopically in nude mice by antiangiogenic mechanisms. *Clin. Cancer Res.* 6, 1936–48.

(52) Harrisson, S., Nicolas, J., Maksimenko, A., Bui, D. T., Mougin, J., and Couvreur, P. (2013) Nanoparticles with in vivo anticancer activity from polymer prodrug amphiphiles prepared by living radical polymerization. *Angew. Chem., Int. Ed. Engl.* 52, 1678–82.

(53) Arya, G., Vandana, M., Acharya, S., and Sahoo, S. K. (2011) Enhanced antiproliferative activity of Herceptin (HER2)-conjugated gemcitabine-loaded chitosan nanoparticle in pancreatic cancer therapy. *Nanomedicine* 7, 859–70.